Quantum Spin Chains and Topology

PH 543: Advanced Statistical Mechanics

Siddhant Midha[*1], Anurag Pendse[†2], and Vatsal[‡3]

[1] *Department of Electrical Engineering, Indian Institute of Technology Bombay*
[2] *Department of Physics, Indian Institute of Technology Bombay*
[3] *Department of Chemistry, Indian Institute of Technology Bombay*

November 27, 2023

Abstract

Contents

[*] siddhantm.iitb@gmail.com
siddhant-midha.github.io

[†] 200260008@iitb.ac.in

[‡] vatsal1005@gmail.com
sites.google.com/iitb.ac.in/vatsal

1 Quantum phase transitions

1.1 Introduction

Before anything else, we must first understand what a Quantum Phase Transition is. Consider a Hamiltonian $H(g)$ whose degrees of freedom reside on the sites of a lattice. Here, g is some dimensionless coupling. We can now follow the evolution of the ground state energy as a function of g. For a finite lattice, the ground state energy is an analytic function of g. However, if g couples to a conserved quantity as $H(g) = H_0 + gH_1$ where H_0 and H_1 commute i.e., $H(g)$ and H_1 commute, we may get an excited state whose energy is equal to the ground state energy i.e., there is a level crossing. This happens as the eigenfunctions of $H(g)$ are independent of g but the eigenvalues are not. Say the excited state energy becomes equal to the ground state energy at $g = g_c$. This creates a point of non-analyticity of the ground state energy as a function of g. However, for a finite lattice, the possibility of avoided crossing is higher. If we consider an infinite lattice, we can get a point of non-analyticity at $g = g_c$ as the avoided crossing becomes sharper and sharper with increasing lattice size. We identify any non-analyticity in the ground state energy as a function of g as a quantum phase transition.
Let Δ represent a scale of characterizing some significant spectral density of fluctuations at zero temperature for $g \neq g_c$. We can consider Δ to be the lowest excitation above the ground state. We have $\Delta \to 0$ as $g \to g_c$. Thus, we can write

$$\Delta \sim J|g - g_c|^{z\nu} \tag{1.1}$$

Here, $z\nu$ is a critical exponent that is usually universal. Along with a vanishing energy scale, we also have a vanishing length scale at the critical point. This correlation length diverges at the critical point as

$$\xi^{-1} \sim \Lambda|g - g_c|^{\nu} \tag{1.2}$$

Here, ν is a critical exponent. We call z the dynamic critical exponent. Λ is an inverse length scale signifying a cutoff in the momentum space. The characteristic energy vanishes as the $-z^{th}$ power of ξ.

$$\Delta \sim \xi^{-z} \tag{1.3}$$

All of the discussion till now refers to singularities in the ground state of the system. Thus, strictly speaking, quantum phase transitions only occur at $T = 0$. However, we can work outwards from the $g = g_c$ and $T = 0$ critical point in order to understand the behavior of the system at any $|g - g_c|$ and T. In some cases, we might have a line of points in the $g - T$ plane where the system undergoes a second order phase transition.

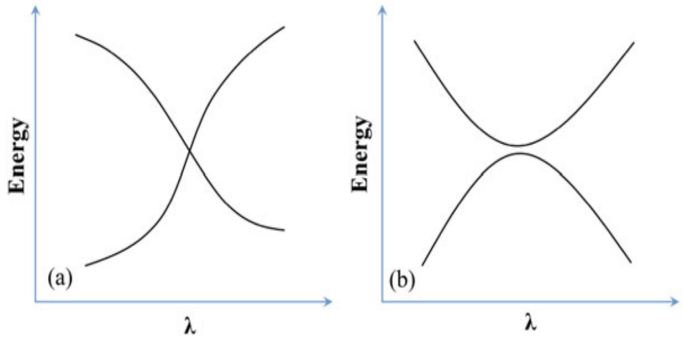

Figure 1: (a) Level crossing and (b) avoided level crossing of the ground state of a quantum Hamiltonian. Figure adapted from [1].

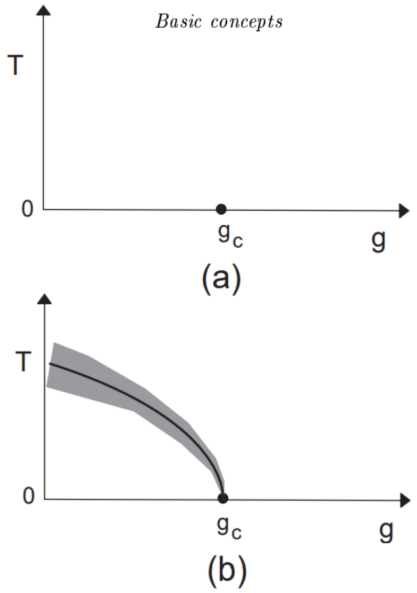

Figure 2: Two possible phase diagrams near a QPT both exhibiting a quantum critical point at $T = 0, g = g_c$: In (a), this is the sole point, and in (b) there is a line of non-zero temperature transitions terminating at $g = g_c$ for $T = 0$, and a classical theory can be applied in the shaded region. Figure adapted from [2]

1.2 Paradigmatic models of QPTs

We follow the discussion in [2].

1.2.1 Quantum Ising model

We begin by writing down the Hamiltonian for the quantum Ising model.

$$H_I = -Jg\sum_i \hat{\sigma}_i^x - J\sum_{\langle ij\rangle} \hat{\sigma}_i^z \hat{\sigma}_j^z \tag{1.4}$$

Here, the tunable H_1 is the first term and this is the term that will give rise to the QPT (Quantum Phase Transition). We have

$$\hat{\sigma}^z = \begin{pmatrix} 1 & 0 \\ 0 & -1 \end{pmatrix} \quad \hat{\sigma}^y = \begin{pmatrix} 0 & -i \\ i & 0 \end{pmatrix} \quad \hat{\sigma}^x = \begin{pmatrix} 0 & 1 \\ 1 & 0 \end{pmatrix} \tag{1.5}$$

These are the Pauli matrices at each site in the lattice. We denote the eigenvalues of each Pauli Matrix simply as $\sigma^{x,y,z}$. As seen from the matrices above,

$$\sigma_i^z = \pm 1 \tag{1.6}$$

Let the eigenvectors of $\hat{\sigma}^z$ be denoted by $|1\rangle$ and $|-1\rangle$ (corresponding to the $+1$ and -1 eigenvalues respectively. Now, the eigenvalues of $\hat{\sigma}^x$ are ± 1 as well. But the eigenvectors are

$$|1_x\rangle = \frac{1}{\sqrt{2}}(|1\rangle + |-1\rangle) \tag{1.7}$$

$$|-1_x\rangle = \frac{1}{\sqrt{2}}(|1\rangle - |-1\rangle) \tag{1.8}$$

In the case that $g = 0$, the model just reduces to the ordinary Ising model as H_I becomes diagonal in the basis of eigenvectors of $\hat{\sigma}^z$.
In the case of $g >> 1$, the first term dominates and to leading order in $\frac{1}{g}$, the ground state is simply

$$|0\rangle = \prod_i |1_x\rangle \tag{1.9}$$

The values of σ^z at two different sites are totally uncorrelated. Thus, we have

$$\langle 0|\, \hat{\sigma}_i^z \hat{\sigma}_j^z\, |0\rangle = \delta_{ij} \tag{1.10}$$

Perturbative corrections in $\frac{1}{g}$ give correlation in σ^z at different locations. We expect

$$\langle 0|\, \hat{\sigma}_i^z \hat{\sigma}_j^z\, |0\rangle \sim e^{\frac{-|x_i - x_j|}{\xi}} \tag{1.11}$$

for some correlation length ξ.
Now, in the other limit where $g << 1$, the nature of the ground state is qualitatively different from that of the other extreme case. Thus, we can conclude that there will be a phase transition at some $g = g_c$ of order unity. In this case, the ground state is a perturbation to the $g = 0$ ground state that is either

$$|1\rangle = \prod_i |1\rangle_i \tag{1.12}$$

or

$$|-1\rangle = \prod_i |-1\rangle_i \tag{1.13}$$

Turning on a small g will flip a small amount of spins. However, the degeneracy will survive due to the global $\mathbb{Z}_2$ symmetry. There is no tunneling matrix between the majority up and the majority down spin states. However, a thermodynamic system will choose a particular gound state. This is known as spontaneous breaking of the $\mathbb{Z}_2$ symmetry. We can characterize the behavior of the correlations as

$$\lim_{|x_i - x_j| \to \infty} \langle 0| \hat{\sigma}_i^z \hat{\sigma}_j^z |0\rangle = N_0^2 \tag{1.14}$$

Here, the ground state is $|\pm 1\rangle$. N_0 is the spontaneous magnetization of the ground state. It is clearly not possible to transform the correlations in the two limits into each other analytically. Thus, there must be a critical point at some $g = g_c$. In the case of a finite lattice, there is a non-zero gap between the ground and first excited state. This gap however vanishes at the critical point.
Before proceeding, let us set $\hbar = 1, k_B = 1$. Let us define the correlator

$$C(x_i, t) = \langle \hat{\sigma}^z(x_i, t) \hat{\sigma}^z(0, 0) \rangle \tag{1.15}$$

We can write this in terms of the partition function as

$$C(x_i, t) = \frac{1}{Z} Tr(e^{-\frac{H_I}{T}} e^{iH_I t} \hat{\sigma}_i^z e^{-iH_I t} \hat{\sigma}_0^z) \tag{1.16}$$

We can introduce an imaginary time τ as $\tau = it$ to get

$$C(x_i, \tau) = \frac{1}{Z} Tr(e^{-\frac{H_I}{T}} e^{H_I \tau} \hat{\sigma}_i^z e^{-H_I \tau} \hat{\sigma}_0^z) \tag{1.17}$$

Define the dynamic structure factor

$$S(k, \omega) = \int dx \int dt C(x, t) e^{-i(kx - \omega t)} \tag{1.18}$$

This is useful as it is directly proportional to the scattering cross section of the neutrons used to probe the material. We can also define a dynamic susceptibility as

$$\chi(k, \omega_n) = \int_0^{\frac{1}{T}} d\tau \int dx C(x, \tau) e^{-i(kx - \omega_n \tau)} \tag{1.19}$$

Here, $\omega_n = 2\pi n T$ is the Matsubara imaginary frequency arising from restricting the periodic functions along the imaginary time axis. We define static susceptibility as

$$\chi(k) = \chi(k, \omega = 0) \tag{1.20}$$

The qualitative properties of the $g > 1.T = 0$ ground state and the $g >> 1, T = 0$ ground state are the same (same goes for the $g < 1, T = 0$ and $g << 1, T = 0$ ground states. Thus, we can investigate the behavior solely in the extreme limits of g.

Let us consider the $g >> 1$ case first. We have already seen the ground state in this case. The lowest excited state can be written as

$$|i\rangle = |-1_x\rangle_i \prod_{j \neq i} |1_x\rangle_j \tag{1.21}$$

To first order in $\frac{1}{g}$, we can neglect the mixing between states of different particle numbers. Due to the $\hat{\sigma}_i^z \hat{\sigma}_{i+1}^z$ term, we get

$$\langle i| H_I |i+1\rangle = -J \tag{1.22}$$

This is because the Ising term is not diagonal in the basis of the x eigenstates. We can go to the momentum space basis as

$$|k\rangle = \frac{1}{\sqrt{N}} \sum_i e^{ikx_j} |j\rangle \tag{1.23}$$

We can now get an additional energy to be added to the ground state energy as

$$\epsilon_k = Jg[1 - \frac{2}{g}\cos(ka) + \mathcal{O}(\frac{1}{g^2})] \tag{1.24}$$

Here, a is the lattice spacing. Thus, the lowest one particle energy state is at

$$\epsilon_0 = 2g - 2J \tag{1.25}$$

Now, we can look at the $g << 1$ limit. As seen before, for the ground state, we have

$$\lim_{|x| \to \infty} = N_0^2 \neq 0 \tag{1.26}$$

The excited states can be described in terms of domain wall excitations. We can look at the domain walls as particles that can hop and form momentum eigenstates and we get

$$\epsilon_k = J(2 - 2g\cos(ka) + \mathcal{O}(g^2)) \tag{1.27}$$

As we will see from the formalism in the next section, i.e., the Jordan-Wigner transformation, we get

$$H_I = \sum_k \epsilon_k (\gamma_k^\dagger \gamma_k - \frac{1}{2}) \tag{1.28}$$

Here, the $gamma_k$ are unitary transformations on the momentum space flipping operators. They act as creation and annihilation operators (note that the form is identical to that in second quantization). We have

$$\epsilon_k = 2J(1 + g^2 - 2g\cos(k))^{\frac{1}{2}} \tag{1.29}$$

We can see that

$$\epsilon_0 = 2J|1 - g| \tag{1.30}$$

Thus, it is evident that $g = 1$ is a critical point.

1.2.2 Quantum Rotor Model

Consider rotors to be places on a d-dimensional lattice. Each rotor has an orientation that is constrained to move on an S^{N-1} where $N > 1$. The orientation of each rotor can be represented by a unit vector $\hat{\mathbf{n}}_i$. We have

$$\hat{\mathbf{n}}_i^2 = 1 \tag{1.31}$$

We can consider each component of this rotor's orientation as its position and define momenta p conjugate to each position coordinate. We now have ($\hbar = 1, k_B = 1$)

$$[\hat{n}_\alpha, \hat{p}_\beta] = i\delta_{\alpha\beta} \tag{1.32}$$

We can work in the components of the angular momentum

$$L_{\alpha\beta} = \hat{n}_\alpha \hat{p}_\beta - \hat{n}_\beta \hat{p}_\alpha \tag{1.33}$$

These are the generators of $SO(N)$. We can define the rotor kinetic energy as

$$H_K = \frac{J\tilde{g}}{2}\hat{\mathbf{L}}^2 \tag{1.34}$$

We can write down the full quantum rotor Hamiltonian as

$$H_R = \frac{J\tilde{g}}{2}\sum_i \hat{\mathbf{L}}_i^2 - j\sum_{\langle ij\rangle} \hat{\mathbf{n}}_i \cdot \hat{\mathbf{n}}_j \tag{1.35}$$

Now, we can give the same argument as we did in the case of the Quantum Ising model, only here, we vary $\tilde{g}$.
For $\tilde{g} >> 1$, we have

$$\langle 0|\, \hat{\mathbf{n}}_i \cdot \hat{\mathbf{n}}_j \,|0\rangle \sim e^{-\frac{|x_i - x_j|}{\xi}} \tag{1.36}$$

For $\tilde{g} << 1$, we have

$$\langle 0|\, \hat{\mathbf{n}}_i \cdot \hat{\mathbf{n}}_j \,|0\rangle = N_0^2 \tag{1.37}$$

We can thus see that a phase transition will occur at some $\tilde{g} = \tilde{g}_c$.

2 More on the TFIM: Topology and Majorana Fermions

2.1 The Jordan-Wigner Transformation

Before we continue to discuss the physics of the QPT in the Ising chain, we review a very useful method of translating the algebra describing a system of spins (or as the kids call them, 'qubits') to the fermionic algebra [3]. Suppose we have a n-spin system over $\mathbb{C}^{2n}$ with the Pauli operators being $\sigma_i^x, \sigma_i^y, \sigma_i^z$ for each $i \in \{1, 2, \ldots, n\}$. We further define,

$$\sigma_i^{\pm} := \frac{\sigma_i^x \pm \iota \sigma_y^n}{2} \tag{2.1}$$

These raising and lowering operators act as $\sigma^+ |\downarrow\rangle = |\uparrow\rangle$ and $\sigma^- |\uparrow\rangle = |\downarrow\rangle$. Further note that the Pauli algebra at a given site satisfies

$$\{\sigma_l, \sigma_k\} = 2\delta_{lk} \forall l, k \in \{x, y, z\} \tag{2.2}$$

leading to

$$\{\sigma^-, \sigma^+\} = 1 \tag{2.3}$$
$$\{\sigma^+, \sigma^+\} = 0 \tag{2.4}$$
$$\{\sigma^-, \sigma^-\} = 0 \tag{2.5}$$

Now, the central idea of the JW mapping is the isomorphism of the up-down state of a spin at site i with the absence or presence of an electron. That is, we identify the spin-up state as a hole, and the spin-down state as a particle,

$$|\uparrow\rangle \sim \circ, \;\; |\downarrow\rangle \sim \bullet \tag{2.6}$$

Thus, we make the loose correspondence of understanding the raising operator as the fermionic creation operator and the lowering operator as the fermionic destruction operator,

$$\sigma^+ \overset{?}{\to} c^\dagger, \;\; \sigma^- + \overset{?}{\to} c \tag{2.7}$$

We recall that the fermionic canonical commutation relations (CCR) read,

$$\{c_i, c_j\} = 0 \tag{2.8}$$
$$\{c_i, c_j^\dagger\} = \delta_{ij} \tag{2.9}$$
$$\{c_i^\dagger, c_j^\dagger\} = 0 \tag{2.10}$$

which are essential to the second quantization formalism widely used to describe fermionic systems and encode the fermionic statistics. But, note that the spin operators satisfy

$$[\sigma_i^-, \sigma_j^+] = [\sigma_i^+, \sigma_j^-] = 0. \tag{2.11}$$

Thus, they would be better interpreted as describing hard-core bosons (hard-core owing to the fact that $\sigma^+ 2 = \sigma^- 2 = 0$). To interpret them as fermions, we need to make sure that the CCR are satisfied. Jordan and Wigner in [4] proposed the following solution:

$$c_i := (\Pi_{j<i}\sigma_i^z)\,\sigma_i^+ \tag{2.12}$$

$$c_i^\dagger := (\Pi_{j<i}\sigma_i^z)\,\sigma_i^- \tag{2.13}$$

Thus, the fermionic algebra is *non-local* in the spin algebra. Moreover, one can easily check that the CCR are now satisfied owing to the string of z operators. This mapping is invertible, and the inverse reads

$$\sigma_i^z = 1 - 2c_i^\dagger c_i \tag{2.14}$$

$$\sigma_i^+ = \Big(\Pi_{j<i}(1 - 2c_j^\dagger c_j)\Big)\, c_i^\dagger \tag{2.15}$$

$$\sigma_i^- = \Big(\Pi_{j<i}(1 - 2c_j^\dagger c_j)\Big)\, c_i \tag{2.16}$$

We then have $\sigma_i^x = \sigma_i^+ + \sigma_i^- = \Big(\Pi_{j<i}(1 - 2c_j^\dagger c_j)\Big)\,(c_i + c_i^\dagger)$.

2.2 JW mapping the Ising chain

Now, consider the TFIM Hamiltonian,

$$\mathcal{H} = -Jg\sum_i \sigma_i^x - J\sum_{\langle ij\rangle}\sigma_i^z\sigma_j^z \tag{2.17}$$

If we rotate the JW frame by 90^o so that $\sigma^z \to \sigma^x$ and $\sigma^x \to -\sigma^z$, then we can write the spin operators using the JW mapping as

$$\sigma_i^x = 1 - 2c_i^\dagger c_i \tag{2.18}$$

$$\sigma_i^z = -\Big(\Pi_{j<i}(1 - 2c_j^\dagger c_j)\Big)\,(c_i + c_i^\dagger) \tag{2.19}$$

While the fermionic expression for σ_i^z is complicated, it turns out that the expression for the product $\sigma_i^z\sigma_{i+1}^z$ is easy to deal with after some algebra, leading to,

$$\sigma_j^z\sigma_{j+1}^z = (c_j^\dagger - c_j)(c_{j+1} + c_{j+1}^\dagger) \tag{2.20}$$

Thus, the JW mapping of the TFIM Hamiltonian is, [5]

$$\mathcal{H} = -JgN + 2gJ\sum_i c_i^\dagger c_i - J\sum_i (c_i^\dagger - c_i)(c_{i+1} + c_{i+1}^\dagger) \tag{2.21}$$

Ignoring the constant term,

$$\mathcal{H} = 2gJ\sum_i c_i^\dagger c_i - J\sum_i (c_i^\dagger c_{i+1} - c_i c_{i+1}^\dagger) - J\sum_i (c_i^\dagger c_{i+1}^\dagger - c_i c_{i+1}) \tag{2.22}$$

This is very similar to the Hamiltonian of the *Kitaev chain*

$$\mathcal{H}_{Kitaev} = -\mu \sum_i c_i^\dagger c_i - t \sum_{\langle ij \rangle} c_i^\dagger c_j - \Delta \sum_i c_i c_{i+1} + h.c. \tag{2.23}$$

where h.c. denotes the harmonic conjugate. The term Δ denotes the order-parameter for p-wave superconducting coupling, creating Cooper pairs on sites $(i, i+1)$ (note, this fermionic model is spinless). This pairing terms emerges naturally from the JW mapping. In fact, for $\Delta = t$, the Kitaev Hamiltonian is *exactly* the Hamiltonian of the JW mapped TFIM. The Kitaev chain exhibits a *topological phase transition* at $\mu = 2t$, which is independent of the value of Δ. Thus, the ferromagnetic to paramagnetic phase transition in the TFIM is exactly the topological phase transition in the Kitaev chain, which happens to be the primary theoretical tool behind the search of *Majorana fermions* for the purpose of topological quantum computation. The phase transition in the Kitaev chain is another example of the ground state QPTs incurring in quantum systems, and we devote the rest of this section to an exploration of the same.

2.3 Spectrum of the Kitaev Chain

. We write down the Hamiltonian again for the purpose of clarity,

$$\mathcal{H} = \sum_i \Big(-\mu(c_i^\dagger c_i - c_i c_i^\dagger) - t(c_i^\dagger c_{i+1} - c_i c_{i+1}^\dagger) + \Delta(c_i^\dagger c_{i+1}^\dagger - c_i c_{i+1}) \Big) \tag{2.24}$$

We analytically compute the spectrum by performing the Fourier transormation, [5]

$$c_j = \frac{1}{\sqrt{N}} \sum_k c_k \exp\{-\iota k j\} \tag{2.25}$$

$$c_j^\dagger = \frac{1}{\sqrt{N}} \sum_k c_k^\dagger \exp\{\iota k j\} \tag{2.26}$$

Then we get, $c_i^\dagger c_i \to c_k^\dagger c_k$, $c_i^\dagger c_{i+1} \to \exp\{-\iota k\} c_k^\dagger c_k$, and $c_i^\dagger c_{i+1}^\dagger \to \exp\{\iota k\} c_k^\dagger c_{-k}^\dagger$. This, with some more algebra gets us,

$$\mathcal{H}_k = \sum_k \Big[(\mu - 2t) c_k^\dagger c_k + \iota \Delta \sin(k)(c_{-k} c_k + c_k^\dagger c_{-k}^\dagger) \Big] \tag{2.27}$$

If I define the vector

$$\Psi_k := \begin{pmatrix} c_{-k} \\ c_k^\dagger \end{pmatrix} \tag{2.28}$$

then this k-space Hamiltonian can be written as,

$$\mathcal{H}_k = \sum_k \Psi_k^\dagger \begin{pmatrix} \mu/2 - t\cos k & -\iota\Delta \sin k \\ \iota \Delta \sin k & -(\mu/2 - t\cos k) \end{pmatrix} \Psi_k \tag{2.29}$$

This is known as the *Bugoliubov-de-Gennes* form, or the BdG trick. We define *Bugoliubov quasiparticle* operators, which are superpositions of electrons and holes, as,

$$\zeta_k := u_k c_k - \iota v_k c_{-k}^\dagger \tag{2.30}$$

which satisfy the ACCRs

$$\{\gamma_k, \gamma_l^\dagger\} = \delta_{kl}, \ \{\gamma_k^\dagger, \gamma_l^\dagger\} = \{\gamma_k, \gamma_l\} = 0 \tag{2.31}$$

Moreover, we can now diagonalize the Hamiltonian as

$$\varepsilon_k = \pm\sqrt{(\mu/2 - t\cos k)^2 + \Delta^2 \sin^2 k} \tag{2.32}$$

The critical point of $g = 1$ in the TFIM corresponds to the $\mu = 2t$ point in the Kitaev chain, and we note that the spectrum becomes gapless at the critical point. Further, near $\mu \approx 2t$, we have,

$$\varepsilon_{crit} \sim |\sin k| \sim k \tag{2.33}$$

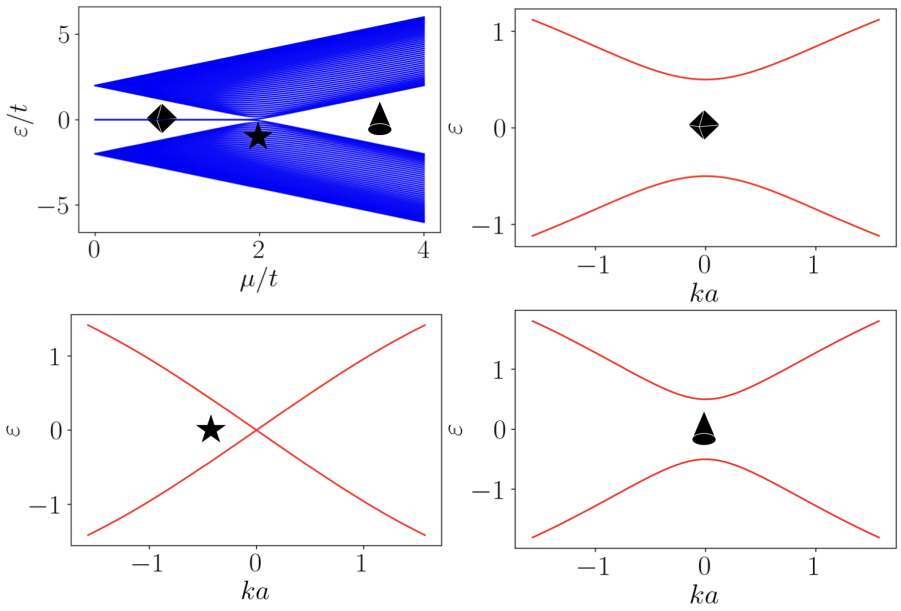

Figure 3: The spectrum and bandstructure of the Kitaev Chain.

giving us the critical exponent $z = 1$ [5]. This is a Dirac cone, and the linearized Dirac Hamiltonian of the Kitaev critical point can be written as $H_{Dirac} = (\mu/2 - t)\tau^z + \Delta\tau^y$, wherein the Dirac cone happens when the mass term $\mu/2 - t \to 0$. We now show the spectrum of the Kitaev chain along with the corresponding band-structures to advance our discussion forward. The results

for a chain of length $N = 40$, with $t = 1$ and $\Delta = 1$ (arb. units) are shown in Fig. 3. Before the critical point $\mu < 2t$, we observe that there exist zero energy states gapped away from the rest of the spectrum, which disappear for $\mu > 2t$. Naturally, we assume this to be the nature of the phase transition, and aim to understand this further. All the while, we see that the band-structure has a Dirac cone at $k = 0$ as shown in $\star$ in Fig. 3. But, we notice something interesting: even though there exist zero energy states before the critical points, the band-structures of the system before and after the critical point shows no such feature. Where did the phase transition disappear? This is where *topology* kicks in. The band-structure is by assumption the property of the *bulk* of the system, and does not account for the boundaries by assuming translational invariance. This points to something obvious albeit powerful: the zero-energy modes must be lying at the *boundary* of our one-dimensional system. How? We now discuss this.

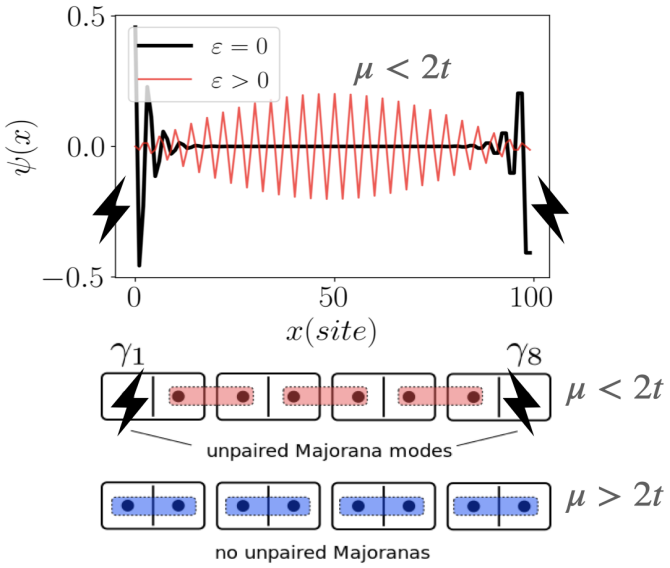

Figure 4: Majorana fermions in the Kitaev chain.

2.4 Majorana zero modes

. We make a transformation without any justification, to be justified soon enough. Let,

$$\gamma_j^+ := c_j^\dagger + c_j; \quad \gamma_j^- := \iota(c_j - c_j^\dagger) \tag{2.34}$$

These define *Majorana fermions*, the algebra for particles which are their own anti-particle, as seen by the fact that $\gamma = \gamma^\dagger$ for $\gamma \in \{\gamma^\pm\}$. Further, one can think of one fermion being split into two Majorana modes through this

transformation. Moreover,

$$c_j = \frac{\gamma_j^+ - \iota\gamma_j^-}{2}; \quad c_j^\dagger = \frac{\gamma_j^+ + \iota\gamma_j^-}{2} \tag{2.35}$$

For the tight-binding chain, arrange the Majorana operators as,

$$\gamma_1, \gamma_2, \ldots, \gamma_{2N-1}, \gamma_{2N} \equiv \gamma_1^+, \gamma_2^-, \gamma_3^+, \gamma_3^-, \ldots, \gamma_N^+, \gamma_N^- \tag{2.36}$$

Thus effectively, we now deal with a Majorana chain of length $2N$. Consider the regime with no edge modes, in the special case of no pairing and no hopping: $\mu > 0$ and $\Delta = 0 = t$. We can write this *unpaired* Hamiltonian by transforming into the Majorana basis as,

$$\mathcal{H}_{unpaired} = (\iota/2)\mu \sum_{i=1}^{N} \gamma_{2i-1}\gamma_{2i} \tag{2.37}$$

In another extreme case, consider the point $\Delta = t$, $\mu = 0$ (thus $\Delta > 0$ and $\mu < 2t$). We can apply the Majorana transformation and then write the *paired* Hamiltonian as,

$$\mathcal{H}_{paired} = \iota t \sum_{i=1}^{N-1} \gamma_{2i+1}\gamma_{2i} \tag{2.38}$$

Note the way of indexing in the sum implies that in the paired case, the Majorana operators γ_1 and γ_{2N} are sitting idle, and not talking to any other γ. On the other hand, in the unpaired case, all the $\gamma_i^\pm$ are coupled at each site i. This is visualized in Fig. 4. This implies two things:

1. The Majoranas $\{\gamma_1, \gamma_{2N}\}$ in the unpaired case effectively encode a non-local fermion. In the thermodynamic limit $N \to \infty$ this implies that information is encoded non-locally.

2. There is a connection between the physics of the theory in the bulk to the behaviour at the boundary. This is called the **bulk-boundary correspondence**.

The first point has to do with why realizations of the Kitaev chain are now the prime candidate for topological quantum computation, where the idea is to encode information non-locally in a robust manner, and perform operations by manipulating the statistics of these Majorana particle. The second is nothing but topology. The topology of the bulk Hamiltonian dictates the presence or absence of zero-energy states at the boundary. The concept of topology can be formalized in the form of Berry phase of the k-space wavefunctions, and can be seen by a winding number of the Bloch Hamiltonian. If one writes the $\mathcal{H}(\mathbf{k})$ as

$$\mathcal{H}(\mathbf{k}) \equiv d(\mathbf{k}) \cdot \vec{\sigma} \tag{2.39}$$

where $\vec{\sigma} = (\sigma^x, \sigma^y, \sigma^z)$ is the Pauli vector, then the presence or absence of edge-modes is dictated by the *winding number* of the $d(\mathbf{k})$ vector as $\mathbf{k}$ circles

around the Brilloin zone. Moreover, for any value of $\mu < 2t$, one is in the so-called topological phase, which is characterized by the presence of robust edge modes. One numerical example for chain of $N = 40$ sites with $\Delta = t = 1$ and $\mu = 1 < 2t$ is shown in Fig. 3. The Majorana mode is shown in black, and a bulk mode for very small $\varepsilon > 0$ is shown in red. The nature of edge-localization in the former and the lack of the same in the latter is clear! The 'robustness' is backed by the fact that the Kitaev chain Hamiltonian exhibits particle-hole symmetry. The PH operator is given as $\mathcal{P} = \tau_x \mathcal{K}$ where $\mathcal{K}$ is complex conjugation. The Kitaev Hamiltonian satisfies $\{\mathcal{H}_{Kitaev}, \mathcal{P}\} = 0$, and this implies that eigenenergies come in pairs of $\pm\varepsilon$. The attempt to move one of the Majorana energies away from zero while the bulk is gapped (which it is!), the PH symmetry gets in the way. The only way to lift the degenerecy would be to couple the edge Majoranas together. But, in the thermodynamic limit this is impossible with a gapped bulk! Hence, the edge-modes are robust, and the next time someone talks to you about topological quantum computing, you can talk right back. Moreover, **at** the critical point, one can see from the Dirac Hamiltonian that the eigenkets will be equal superpositions of electrons and holes, which are then free to propagate along the rest of the chain owing to the gap closing at the Dirac cone. This is what makes the transition happen: the zero-energy states now become gapped bulk modes for $\mu > 2t$.

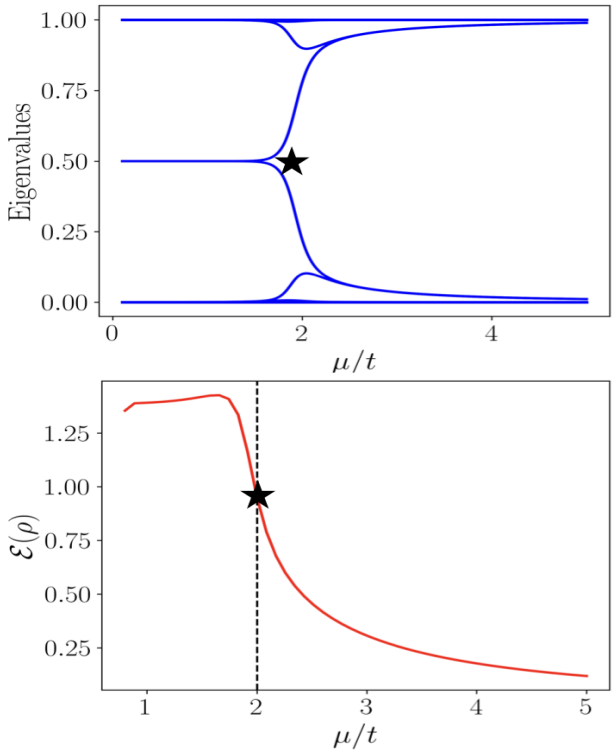

Figure 5: Entanglement in the Kitaev chain.

2.5 Entanglement in quantum phase transitions

. We wrap up this discussion by discussing how an inherently quantum mechanical quantity, the entanglement, which may be thought of as correlations beyond what is possible classically, manifests in QPTs. This question is quite natural, owing to the fact that quantum phase transitions are intimately linked to a reconstruction of the low-lying states of the Hamiltonian. At $T = 0$, as we have discussed, there does not exist a thermal energy scale, and thus all fluctuations are quantum mechanical, and not thermal. It is thus natural to ask how entanglement can help us understand QPTs. Indeed, coupled with the recent developments in the areas of quantum information and computation, there have been significant research efforts in using entanglement and related quantities like quantum discord, coherent information, quantum fidelty have been used to study QPTs [1]. This becomes even more important when classifying multistate systems, wherein one needs a separate order parameter for each state. Even more generally, the traditional method of studying phase transitions under the umbrella of Landau-Ginzburg's spontaneous symmetry-breaking does not work for Berezinskii-Kosterlitz-Thouless transition or topological phase transitions owing to the lack of a local order parameter or symmetry-breaking. As it hap-

pens, we were *coincidently* dealing with a topological phase transition in this section! So let us conclude with a discussion about the nature of entanglement in this transition.

The central quantity of interest here is quantum entanglement. But, there exist numerous ways of quantifying entanglement, and given the finiteness of this document we must stick to one. We stick to the *von-Neumann entanglement entropy* (just EE), which for a bipartite, thus consisting of systems $A-B$, **pure** state is given by

$$\mathcal{E}(|\Psi\rangle) = -Tr[\rho_A \log \rho_A] = S(\rho_A) \tag{2.40}$$

where $\rho_A := Tr_B[|\Psi\rangle \langle\Psi|]$ is the partial trace over subsystem B. The central idea is that, if the *reduced* state has uncertainity, quantified by the entropy $S(\rho_A) > 0$ then there must be quantum correlations between $A - B$. For instance, for the Bell-state

$$|\Phi\rangle = \frac{|00\rangle + |11\rangle}{\sqrt{2}} \tag{2.41}$$

we have that $\rho_A = I/2$ and $S(\rho_A) = \log 2$, which is the maximal value of the entropy function for a single qubit. Thus, the Bell-state is maximally entangled as postulated. Now, in our formulation, we have the Hamiltonian $\mathcal{H}_{Kitaev}$ and are interested in computing the EE of the ground state. One method to do this is via the *correlation matrix* of the Hamiltonian, which consists of the following terms

$$\langle c_i^\dagger c_j \rangle = \langle \Psi | c_i^\dagger c_j | \Psi \rangle \tag{2.42}$$

In this method, one computes the reduced correlation matrix of the subsystem A, denoted as $\mathcal{C}_A$ and one has that [6]

$$\mathcal{E}(|\Psi\rangle) = -Tr[\rho_A \log \rho_A] = S(\rho_A) = -\sum_i \zeta_i \log \zeta_i - (1-\zeta_i) \log (1-\zeta_i) \tag{2.43}$$

where, ζ_i is the eigenspectrum of the reduced correlation matrix $\mathcal{C}_A$. This is also called the *entanglement spectrum* of the quantum system, and also provides valuable information. We defer a discussion of the details of this to [6] and references therein. We now discuss these quantities for the Kitaev chain. The results are shown in Fig. 5. The first plot shows the entanglement spectrum and the second plot shows the entanglement entropy computed from the former spectrum. We see that, at the critical point $\mu = 2t$ the entanglement spectrum changes from having a value at $1/2$ to values at 0 and 1. Note that if $f(x) := -x \log x - (1-x) \log (1-x)$ then $f(0) = f(1) = 0$ and $f(1/2) = \log 2$. Thus, the mode of the eigenvalues at $\zeta = 0.5$ before the QPT signifies a non-zero contribution to the entropy owing to $f(1/2)$ in Eq. 2.43, and whenever the reduced correlation matrix has eigenvalues in $\{0, 1\}$ the entanglement is zero. Thus, the critical point manifests as a change in the entanglement spectra, which is non-analytic in the thermodynamic limit. What is the physical meaning of this? We already discussed that for $\mu < 2t$, we have a pair of paired Majorana modes **separated** from each other. This pairing is what contributes a unit

of $2 \log 2$ entanglement in the $\mu < 2t$ phase, conveying that that the chain is **area-law entangled**, with two entanglement modes supported on the edges. This is how such a simple model illustrates rich physics: starting from the TFIM, with the JW Mapping and the fermionic interpretation, with topology and entanglement, such models are a workhorse of theoretical understanding of many concepts of many-body physics, phase transitions, and entanglement theory. We encourage the interested reader to further study [1] to delve deeper into these concepts.

We now discuss the idea of quantum to classical mapping in the next section, and conclude the report with some examples of the same.

3 Quantum to classical mapping

3.1 Formalism: Lattice field theories

The natural language of many-particle quantum mechanics is that of fields (second quantization), but the exact continuum theories are ridden with unpleasant infinities. A remedy for this is to discretize the fields over a lattice with finite spacing of points, which is also a necessity for any numerical computation. The formal, exact theory is reproduced on approaching the continuum limit of such lattice theories. It turns out that a lattice discretization of field theories regularizes the continuum theories, i.e. gets rid of the divergences, and it does so non-perturbatively, making the methods effective even at strong coupling [7]. Lattice field theories map a $(1, d)$-dimensional quantum field theory (QFT) to a $(d + 1)$-dimensional classical statistical field theory.

Regulating continuum QFTs through a lattice discretization requires a tuning parameter to be set as a threshold, like lattice spacing a as the cutoff for space(time) separation in the minimum, or the corresponding momentum cutoff $\hbar/a$ in the maximum. Latticization involves choosing a lattice and expressing derivatives as finite differences. Lattice spacing corresponds to the correlation length of the lattice system that tells how fast the correlation functions vanish.

There are two approaches to discretization,

- discretizing both space and time;
- or only discretizing space for fixed continuum-time spatial slices of the spacetime manifold (also known as the Hamiltonian formalism).

3.1.1 Motivation to study finite-temperature theories

Quantum statistical mechanics for the many-body problem can most conveniently be accessed through the grand canonical ensemble, with the grand partition function,

$$\mathcal{Z}_q(\beta, \mu) = \mathrm{Tr}\Big\{e^{-\beta \hat{K}}\Big\}, \tag{3.1}$$

where $\hat{K} = \hat{H} - \mu\hat{N}$, $\hat{H}$ is the Hamiltonian, $\hat{N}$ is the number operator and the trace is defined over the whole of the Hilbert space of the problem ($\sum_m \langle m|\cdots|m\rangle$).

As tough as achieving a near-maximal span of the low-energy subspace of Hilbert space is for the conventional zero-temperature ground-state theories, a thermal many-particle theory requires a good description of the excited states in the Hilbert space, the knowledge of which eludes our current theoretical and computational technology, rendering us unable to carry out such a trace as in equation (3.1). All attempts to provide a viable Hilbert space description for a finite-temperature many-body theory are thus, essentially exercises in circumventing this trace operation through clever ansatze [8].

3.1.2 Path integral formulation of quantum mechanics

The probability amplitude for a particle to travel from (x_i, t_i) to (x_f, t_f) is given by the inverse propagator (or kernel),

$$K(x_f, t_f; x_i, t_i) = \int \mathcal{D}\left[x(t)\right] e^{\frac{i}{\hbar} S[x(t)]}, \tag{3.2}$$

where $S[x(t)]$ is the action functional over classical trajectories (or paths) $x(t)$ and the integral measure goes as $\sim \prod_j \mathrm{d}x(t_j)$ (with appropriately defined factors), making (3.2) some sort of a "sum over paths". This is equivalent to the wavefunction formalism ($\{E_n, \phi_n\}$),

$$K(x_f, t_f; x_i, t_i) = \sum_n e^{\frac{i}{\hbar} E_n (t_f - t_i)} \phi_n^*(x_f) \phi_n(x_i). \tag{3.3}$$

As a generating functional for correlation functions, the "vacuum-to-vacuum" amplitude, or partition function, is given by,

$$Z = \int \mathcal{D}\left[\{\phi\}\right] e^{\frac{i}{\hbar} S(\{\phi\})}. \tag{3.4}$$

Introducing an auxiliary function $J(x)$, we define our generating functional as,

$$Z[J] = \int \mathcal{D}\left[\{\phi\}\right] \exp\left\{ \frac{i}{\hbar} \left[S(\{\phi\}) + \int_{x_i}^{x_f} \mathrm{d}^4 x \, J(x)\phi(x) \right] \right\}. \tag{3.5}$$

The n-point correlation functions are then given by the functional derivatives,

$$G_n(x_1, \ldots, x_n) = (-i\hbar)^n \frac{1}{Z[0]} \left. \frac{\delta^{\mathrm{n}} Z}{\delta J(x_1) \cdots \delta J(x_n)} \right|_{J=0}. \tag{3.6}$$

Partition functions of QFTs are considered to be imaginary-time versions of statistical mechanical partition functions, as the highly oscillatory e^{iS_M} in (3.4) (where S_M denotes the action in Minkowski spacetime) is Wick-rotated into a damping exponential e^{-S_E}, where S_E denotes the Euclidean action, i.e. as,

$$t \to -i\tau, \qquad S_M \to iS_E, \qquad e^{iS_M} \to e^{-S_E}, \qquad \tau \in [0, \beta]. \tag{3.7}$$

For numerical realizations, this is a crucial step as the oscillatory e^{iS_M} can lead to numerical instabilities.

Upon euclideanization and discretization, the vacuum-to-vacuum amplitude takes the form,

$$Z \sim \int \prod_j \mathrm{d}\phi_j \, e^{-S_E(\{\phi_j\})}, \tag{3.8}$$

which resembles the classical statistical mechanical partition function.

Thus the partition function in (3.4) can be understood as a sum of "transition" amplitudes, but in the Euclidean imaginary time evolution,

$$\begin{aligned} Z &= \mathrm{Tr}\Big\{ e^{-\beta(\hat{H}-\mu\hat{N})} \Big\} \\ &= \sum_a \int \mathcal{D}\left[\phi_a\right] \, \langle \phi_a | e^{-\beta(\hat{H}-\mu\hat{N})} | \phi_a \rangle \,, \end{aligned} \tag{3.9}$$

with the periodic boundary condition $\phi(x,0) = \phi(x,\beta)$.

Hence, from the above discussion it is clear how a dynamics problem (QFT with real-time evolution) was mapped into a statics problem (classical statistical mechanics with imaginary-time evolution) through latticization, and the partition function for a QFT in (3.4) does not give a transition probability in the real time like the kernel of quantum mechanics (3.2) does, leaving it to describe just the vacuum-to-vacuum transition amplitudes (bubble diagrams in a perturbative series), or in the statistical mechanical language, the equilibrium properties of the system. Wick rotation (3.7) enables us to identify imaginary time $\tau/\hbar$ of the lattice field theory with inverse temperature β of the classical statistical mechanical system, which completes the quantum to classical mapping of the problem.

3.1.3 The classical limit of quantum statistical mechanics

The quantum partition function for a free particle of mass m in a potential $V(x)$ in the imaginary-time formalism is written as [9],

$$Z(\beta) = \int \mathrm{d}x \int_x^x \mathcal{D}\left[x\right] \exp\left\{ -\frac{1}{\hbar} \int_0^{\beta\hbar} \mathrm{d}\tau \left(\frac{m}{2} \left(\frac{\mathrm{d}x}{\mathrm{d}\tau} \right)^2 + V[x(\tau)] \right) \right\}, \tag{3.10}$$

where the path (functional) integral is over all possible closed paths. This is the reason why we only obtain finite-temperature corrections to equilibrium properties in the imaginary-time formalism, instead of any real-time non-equilibrium dynamics. These show up as bubble diagrams in a diagrammatic expansion of cluster operators.

Considering the "classical" limit, $\beta\hbar \to 0$, the kinetic energy for a particle to return to its starting position x, having been displaced by Δx, in $\beta\hbar$ time is of the order $\frac{m}{2}\left(\frac{\Delta x}{\beta\hbar}\right)^2$. The Boltzmann factor then becomes of the order,

$$\sim \exp\left\{ -\frac{1}{\hbar} \left(\frac{\Delta x}{\beta\hbar} \right)^2 \beta\hbar \right\}. \tag{3.11}$$

In this small time limit, all Δx incursions must be exponentially suppressed,

i.e.,

$$\Delta x \sim \sqrt{\frac{\beta}{m}}\hbar. \tag{3.12}$$

This is called the *thermal wavelength*. Assuming the potential to be varying over length scales appreciably bigger than Δx, we can approximate (3.10) by,

$$\begin{aligned} Z(\beta) &\sim \int \mathrm{d}x\, e^{-\beta V(x)} \int_x^x \mathcal{D}\left[x\right] \exp\left\{ -\frac{1}{\hbar} \int_0^{\beta\hbar} \mathrm{d}\tau\, \frac{m}{2} \left(\frac{\mathrm{d}x}{\mathrm{d}\tau}\right)^2 \right\} \\ &= \int \mathrm{d}x\, e^{-\beta V(x)} \sqrt{\frac{m}{2\pi\beta\hbar^2}}, \end{aligned} \tag{3.13}$$

where the last equality follows from the transition amplitude for a free particle,

$$W(q_s, t_s, q_t, t_t) = \sqrt{\frac{m}{2\pi i\hbar(t_t - t_s)}}\, e^{\frac{i}{\hbar}\frac{m(q_t - q_s)^2}{2(t_t - t_s)}}. \tag{3.14}$$

Compare this with the classical partition function,

$$\begin{aligned} Z &= A \int \mathrm{d}x \int \mathrm{d}p\, \exp\left\{ -\beta \left(\frac{p^2}{2m} + V(x) \right) \right\} \\ &= A \sqrt{\frac{2\pi m}{\beta}} \int \mathrm{d}x\, e^{-\beta V(x)}. \end{aligned} \tag{3.15}$$

Comparing (3.13) and (3.15), we have that,

$$A = \frac{1}{2\pi\hbar}, \tag{3.16}$$

which explains the origin of the deceptively spurious pre-factor of $\hbar$ to the classical partition function, which corresponds to the fundamental uncertainty in the definition of a $\mathrm{d}x\,\mathrm{d}p$ region of the classical phase space, and thereby the number of classical states within that region.

3.2 Illustration

3.2.1 Classical to quantum: 1D Ising model

We will see how the statistical mechanics of a 1D classical Ising chain maps onto the behavior of a single quantum Ising spin. Let T_1 and T_2 be the transfer matrices due to the Ising interaction and the magnetic field interaction respectively. With an Ising coupling of K, we get

$$T_1 = e^K (1 + e^{-2K} \hat{\sigma}^x) \tag{3.17}$$

$$T_2 = e^{a\tilde{h}\hat{\sigma}^z} \tag{3.18}$$

We further get

$$T_1 \approx e^{a(-E_0 + \frac{1}{2\xi}\hat{\sigma}^x)} \tag{3.19}$$

We now get

$$T_1 T_2 = e^{-aH_Q} \tag{3.20}$$

$$Z = (T_1 T_2)^M \approx Tr(e^{\frac{-H_Q}{T}}) \tag{3.21}$$

Here,

$$H_Q = E_0 - \frac{\Delta}{2}\hat{\sigma}^x - \tilde{h}\hat{\sigma}^z \tag{3.22}$$

Here,

$$\Delta = \frac{1}{\xi} \tag{3.23}$$

We can clearly see that this is the Hamiltonian for a single Ising spin. This will lead to identical correlators as well.

References

[1] A. Bayat, S. Bose, and H. Johannesson, eds., *Entanglement in Spin Chains: From Theory to Quantum Technology Applications*, en, Quantum Science and Technology (Springer International Publishing, Cham, 2022), https://link.springer.com/10.1007/978-3-031-03998-0 (visited on 11/27/2023).

[2] S. Sachdev, *Quantum phase transitions*, 2nd ed. (Cambridge University Press, 2011).

[3] M. A. Nielsen, "The Fermionic canonical commutation relations and the Jordan-Wigner transform", en,

[4] *Über das Paulische äquivalenzverbot — Zeitschrift für Physik A Hadrons and nuclei*, https://link.springer.com/article/10.1007/BF01331938 (visited on 11/26/2023).

[5] K. Chhajed, "From Ising model to Kitaev Chain – An introduction to topological phase transitions", Resonance **26**, arXiv:2009.01078 [cond-mat], 1539–1558 (2021), http://arxiv.org/abs/2009.01078 (visited on 11/26/2023).

[6] A. Kejriwal and B. Muralidharan, "Nonlocal conductance and the detection of Majorana zero modes: Insights from von Neumann entropy", Physical Review B **105**, Publisher: American Physical Society, L161403 (2022), https://link.aps.org/doi/10.1103/PhysRevB.105.L161403 (visited on 11/27/2023).

[7] N. Hari Dass, "Field theories on a lattice", Pramana **25**, 439–446 (1985).

[8] S. H. Mandal, G. Sanyal, and D. Mukherjee, "A thermal cluster-cumulant theory", in *Microscopic quantum many-body theories and their applications* (Springer, 1998), pp. 93–117.

[9] R. Shankar, *Quantum field theory and condensed matter: an introduction* (Cambridge University Press, 2017).